

Concentrative nucleoside transporter 1 (hCNT1) promotes phenotypic changes relevant to tumor biology in a translocation-independent manner

S Pérez-Torras^{*1}, A Vidal-Pla¹, P Cano-Soldado¹, I Huber-Ruano¹, A Mazo^{1,2} and M Pastor-Anglada^{*1,2}

Nucleoside transporters (NTs) mediate the uptake of nucleosides and nucleobases across the plasma membrane, mostly for salvage purposes. The canonical NTs belong to two gene families, SLC29 and SLC28. The former encode equilibrative nucleoside transporter proteins (ENTs), which mediate the facilitative diffusion of natural nucleosides with broad selectivity, whereas the latter encode concentrative nucleoside transporters (CNTs), which are sodium-coupled and show high affinity for substrates with variable selectivity. These proteins are expressed in most cell types, exhibiting apparent functional redundancy. This might indicate that CNTs have specific roles in the physiology of the cell beyond nucleoside salvage. Here, we addressed this possibility using adenoviral vectors to restore tumor cell expression of hCNT1 or a polymorphic variant (hCNT1S546P) lacking nucleoside translocation ability. We found that hCNT1 restoration in pancreatic cancer cells significantly altered cell-cycle progression and phosphorylation status of key signal-transducing kinases, promoted poly-(ADP-ribose) polymerase hyperactivation and cell death and reduced cell migration. Importantly, the translocation-defective transporter triggered these same effects on cell physiology. Moreover, this study also shows that restoration of hCNT1 expression is able to reduce tumor growth in a mouse model of pancreatic adenocarcinoma. These data predict a novel role for a NT protein, hCNT1, which appears to be independent of its role as mediator of nucleoside uptake by cells. Thereby, hCNT1 fits the profile of a transceptor in a substrate translocation-independent manner and is likely to be relevant to tumor biology.

Cell Death and Disease (2013) 4, e648; doi:10.1038/cddis.2013.173; published online 30 May 2013

Subject Category: Cancer

Nucleosides have important physiological roles as nutrients and metabolites and are crucial for the control of cell and tissue growth. For nucleosides to exert their physiological effects, specific membrane transporters that mediate their flux across cell membranes are required. Nucleoside transporters (NTs) are integral membrane proteins implicated in the salvage of natural nucleobases and nucleosides for nucleic acid synthesis. NTs belong to solute carrier families 28 and 29 (SLC28 and SLC29), which encode concentrative nucleoside transporters (CNT) and equilibrative nucleoside transporter proteins (ENTs), respectively. ENTs facilitate transport of substrates down their concentration gradient, whereas CNTs mediate the unidirectional flow of substrates in an active, sodium-coupled manner. Remarkably, transport proteins with overlapping or even identical substrate selectivity are coexpressed in mammalian cells. In humans, hENT1 and hENT2 exhibit low affinity and broad permeant selectivity, transporting both purine and pyrimidine nucleosides. Nevertheless,

CNTs differ in their substrate selectivity, whereas hCNT1 and hCNT2 accept only pyrimidine and purine nucleosides, respectively (with the exception of uridine, which is translocated by all SLC28 members), hCNT3 accepts both purines and pyrimidines as substrates.^{1–3} CNT proteins, and hCNT1 in particular, are broadly detected in epithelia, although their expression is often low to negligible in undifferentiated states, as reported for intestinal crypt cells, fetal hepatocytes and human tumors.^{4–8} hCNT1 shows complex regulation by insulin in cardiac fibroblasts⁹ and by hepatocyte nuclear factor (HNF)-4, bile acids,¹⁰ tumor necrosis factor (TNF)- α and interleukin (IL)-6¹¹ in hepatocytes; its expression also appears to be cell cycle dependent, showing upregulation at the S phase.¹² Most tumor-derived cell lines show low or even undetectable hCNT1 expression, although their normal counterparts normally express this membrane protein. Such is the case, for instance, for pancreatic adenocarcinoma and breast cancer.^{6,7} Nevertheless, ENTs may be considered

¹Department of Biochemistry and Molecular Biology, Institute of Biomedicine, University of Barcelona and National Biomedical Research Institute of Liver and Gastrointestinal Diseases (CIBERehd), Barcelona, Spain

*Corresponding author: M Pastor-Anglada or S Perez-Torras, Departament de Bioquímica i Biologia Molecular, Institut de Biomedicina, Universitat de Barcelona and National Biomedical Research Institute of Liver and Gastrointestinal Diseases (CIBERehd), Diagonal 643, Barcelona 08028, Spain. Tel: +34 934 021 543; Fax: +34 934 021 554; E-mail: mpastor@ub.edu or s.perez-torras@ub.edu

²These authors contribute equally to this work.

Keywords: hCNT1; nucleoside transporter; cell signaling; transceptor

Abbreviations: hCNT1, human concentrative nucleoside transporter; NT, nucleoside transporter; ENT, equilibrative nucleoside transporter; SLC, solute carrier; PARP, poly-(ADP ribose) polymerase; MOI, multiplicity of infection; RT-PCR, reverse transcription-PCR; ERK, extracellular regulated kinase; AIF, apoptosis-inducing factor; HNF-4, hepatocyte nuclear factor 4; TNF- α , tumor necrosis factor α ; mTOR, mammalian target of rapamycin; CREB, cAMP-response element-binding protein; GPCR, G-protein-coupled receptor; PDK1, phosphoinositide-dependent kinase 1

Received 28.2.13; revised 18.4.13; accepted 22.4.13; Edited by A Stephanou

ubiquitous transporters, although with significant variability in tissue abundance.¹³ ENT1 expression is mostly linked to cell proliferation^{14,15} and is highly retained in tumors.^{8,16,17} Thus, it appears that most tumor cells rely upon the low affinity, broad selectivity hENT1 to supply nucleosides for salvage and proliferation purposes.

We hypothesized that hCNT-type proteins, and hCNT1 in particular, have specific roles in the physiology of the cell beyond mere nucleoside salvage; if validated, this would help to explain apparent redundancies in transporter expression. To test this possibility, we monitored changes in cell physiology and cell cycle-related events produced by restoration of hCNT1 expression in tumor cells lacking hCNT1 function. These studies revealed a biological function for hCNT1 that appears to be independent of its well-characterized nucleoside translocation role, providing the first evidence that a NT protein transduces signals to the cell interior and thus, acts as a transceptor.

Results

Validation of AdhCNT1 function. The adenoviral vector AdhCNT1 was generated as a tool for overexpressing hCNT1 in a wide variety of cell lines. In order to examine its efficacy in inducing hCNT1-related function, we infected a panel of tumor cell lines with AdhCNT1 and the control adenovirus, Adctrol, at different multiplicities of infection (MOIs) and determined sodium-dependent cytidine uptake

48 h after infection. At the tested MOIs, cytidine uptake increased in a dose-dependent manner, whereas no hCNT1-related activity was observed after Adctrol infection of NP-9 cells, although NP-29 cells, when transduced with the empty vector did show some minimal Na⁺-coupled cytidine uptake (Figure 1a and Supplementary Figure S1). The pancreatic adenocarcinoma cell lines, NP-9 and NP-29, were chosen for further characterization of the effects of hCNT1 overexpression on several aspects of tumor cell biology. In both cell lines, infection with hCNT1 induced a dose-dependent increase in cytidine uptake (Figure 1a). hCNT1 mRNA, determined by quantitative reverse transcription-PCR (RT-PCR), was similarly increased in both cell lines in a dose-dependent manner 48 h after cDNA transduction (Figure 1b), resulting in a corresponding increase in the total amount of hCNT1 protein (Figure 1c). Under these conditions, no relevant changes in the mRNA levels of the endogenously expressed NTs, hENT1 and hENT2, were observed (Supplementary Figure S2).

hCNT1 expression alters the cell-cycle profile and induces non-apoptotic cell death. Unexpectedly, AdhCNT1 infection altered cell morphology and viability in both NP-9 and NP-29 cell lines, changes that were dose- and time-dependent (Figure 2a) and consistent with the induction of cell death. Interestingly, these changes were observed at the lowest MOI used (Figure 2a). These unexpected changes prompted us to analyze the cell-cycle profile 48 h after

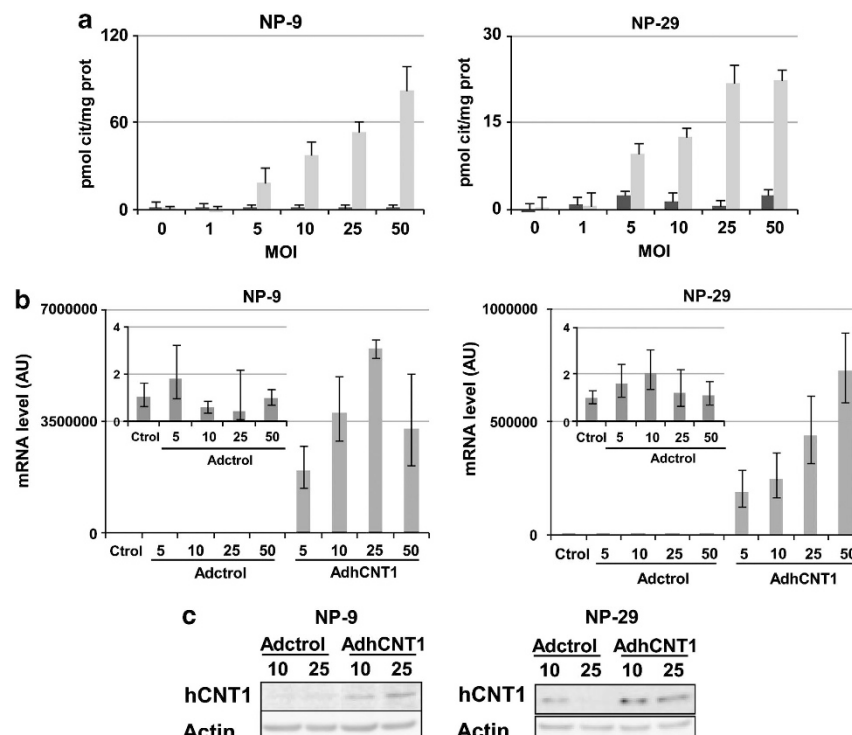


Figure 1 Functional characterization of AdhCNT1. NP-9 and NP-29 cells were infected with AdhCNT1 or Adctrol at different MOIs, and all parameters were analysed 48 h post-infection. (a) hCNT1 sodium-dependent uptake of [³H]cytidine, calculated as uptake in NaCl medium minus uptake in choline chloride, measured in cells transduced with Adctrol (black bars) or AdhCNT1 (gray bars). Results are expressed as means ± S.E.M. and correspond to a representative experiment (*n* = 3). (b) Relative amounts of hCNT1 mRNA determined by RT-PCR. The graphics correspond to a representative experiment (*n* = 3), and the error bars indicate the range of possible values define by the S.E.M. of the delta threshold cycles. (c) Western blot analysis of hCNT1 expression

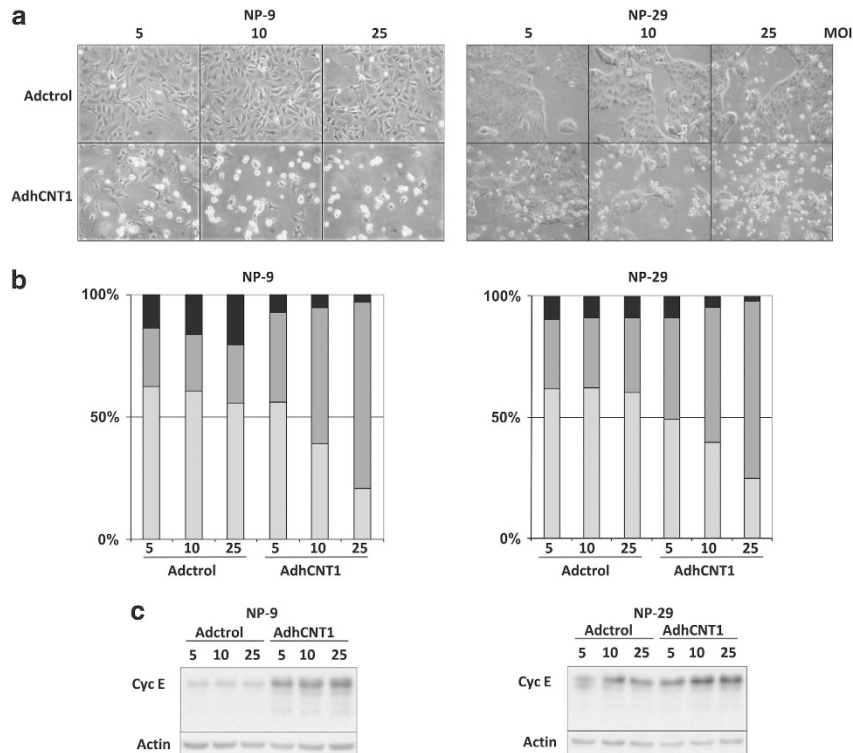


Figure 2 hCNT1 overexpression alters cell morphology and cell-cycle profile. All parameters were analysed in cells infected with Adctrol or AdhCNT1. (a) Morphology of pancreatic tumor cells after infection with Adctrol or AdhCNT1 at different MOIs. Pictures were taken on day 3 (NP-9) or 4 (NP-29) after infection. (b) G1 (gray), S (dark gray) and G2 (black) phases were quantified by flow cytometric analysis of propidium iodide-stained cells 48 h after infection. The graphic corresponds to a representative experiment ($n = 3$). (c) Western blot analysis of cyclin E expression 48 h after infection at different MOIs

hCNT1 transduction. In both cell lines, overexpression of hCNT1 led to a dose-dependent accumulation of cells in S phase (Figure 2b). At the highest dose (25 MOI), the number of cells in S phase increased to $> 70\%$ above control values in both cell lines (Figure 2b). Under the same conditions, no significant changes in cell-cycle profiles were observed in cells infected with Adctrol. Moreover, in both cell lines, cell-cycle alterations correlated with an increase in cyclin E expression (Figure 2c), which typically reached a peak at the G1–S transition.

To further investigate the nature of the cell death that occurred after hCNT1 overexpression, we analyzed cells for annexinV binding and immunoblotted for PARP (poly (ADP-ribose) polymerase). In the first set of experiments, NP-9 and NP-29 cells were infected with AdhCNT1 or Adctrol at different MOIs, and annexinV binding was determined at different times post-infection. Both cell lines showed clear induction of cell death, especially at higher MOIs (Figure 3a; 96 h for NP-9 and 72 h for NP-29). However, no annexinV-positive/propidium iodide-negative cells, indicative of apoptosis, were observed under any assay conditions, arguing against induction of apoptosis. Moreover, PARP cleavage was not detected 48 or 72 h after infection with AdhCNT1 (Figure 3b), ruling out late apoptosis. However, unexpectedly, both cell lines showed a smear of higher molecular weight bands suggestive of PARP hyperactivation, which was subsequently confirmed by an observed increase in poly(ADP-ribose) polymers (Figure 3b). Over-activation of

PARP-1 leading to the nuclear translocation of AIF (apoptosis-inducing factor) is a defining feature of parthanatos, a unique form of PARP-1-dependent cell death characterized by toxic accumulation of PAR in the cytosol following the over-activation of PARP-1. However, nuclear AIF was not detected after hCNT1 transduction (Figure 3c), suggesting that hCNT1 overexpression does not cause this type of cell death.

hCNT1 expression prevents subcutaneous tumor growth. The observations described above prompted us to evaluate the potential antitumor activity of hCNT1 *in vivo*. To this end, we injected pre-established, NP-9-derived subcutaneous tumors in nude mice with AdhCNT1 or Adctrol and monitored subsequent tumor growth. AdhCNT1 infection at 2×10^8 transducing units (TU) per tumor induced a significant antitumoral response that was evident after the first treatment, considerably reducing tumor volume (422 and 975 mm³ in AdhCNT1- and Adctrol-infected tumors, respectively) by the end of the experiment (Figure 4a). Consistent with this, tumor weight was also significantly reduced ($> 50\%$) at this time (Figure 4b). A macroscopic analysis of the interior of hCNT1-overexpressing tumors revealed a necrotic appearance (Figure 4c).

hCNT1 expression modulates intracellular signaling pathways. At this point, we hypothesized that restoration of hCNT1 function in tumor cells would evoke changes in cell physiology. We further addressed this by examining the

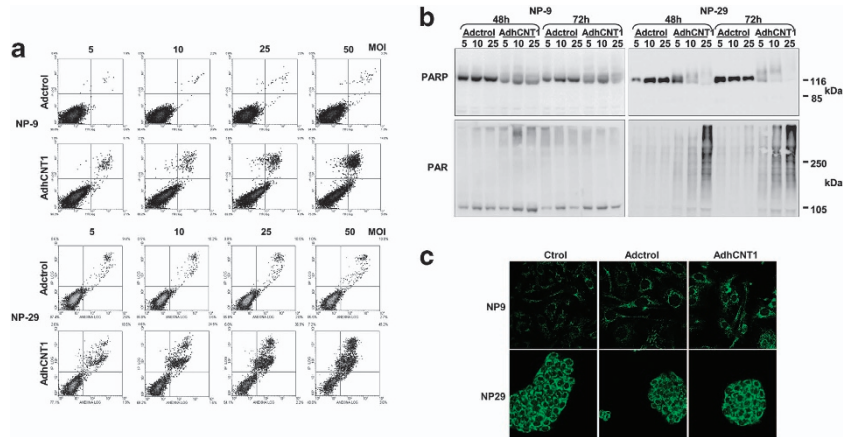


Figure 3 hCNT1 induces non-apoptotic cell death. NP-9 and NP-29 cells were infected with Adctrol or AdhCNT1. (a) Annexin binding was determined 72 (NP-9) or 96 (NP-29) h after infection at different MOIs. (b) Total cell extracts obtained 48 and 72 h after infection at different MOIs were immunoblotted for PARP and PAR. (c) AIF expression was analysed immunocytochemically 48 h after infection at an MOI of 10. Magnification, $\times 63$

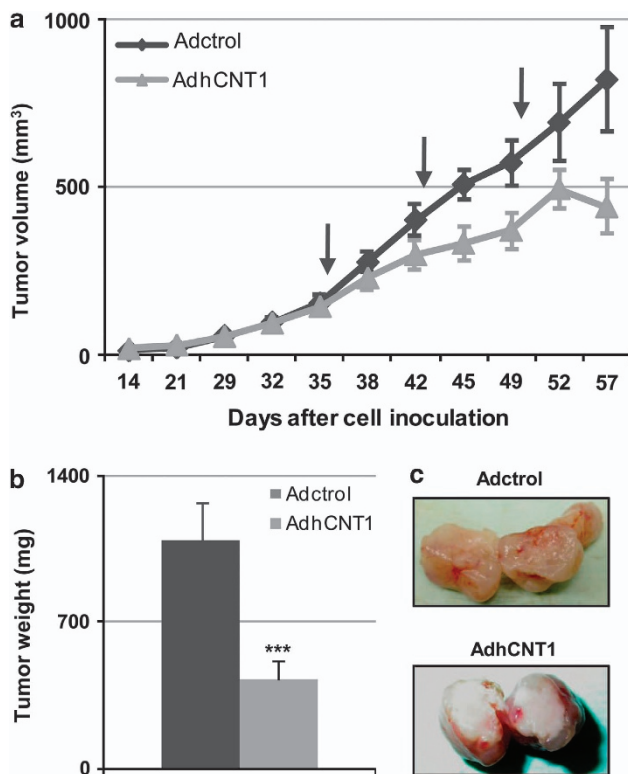


Figure 4 hCNT1 inhibits tumor growth. Xenografts were generated by subcutaneous injection of NP-9 cells. Once tumors reached a volume of 90 mm^3 , adenoviruses were delivered once a week by intratumoral injection for 3 weeks (marked with arrows). (a) Tumor volume was measured at the indicated time points. Adctrol and AdhCNT1 are represented in black and gray, respectively. Data are means \pm S.E.M. ($n = 7-10$ tumors). (b) Tumor weight was measured on the day of harvest after excision from the euthanized mouse. Bars are means \pm S.E.M. ($n = 7-10$ tumors). Statistical significance was determined with Student's *t*-test; $***P < 0.005$. (c) Macroscopic images of the interiors of excised tumors

impact of hCNT1 expression on the basal phosphorylation profiles of a panel of kinases implicated in a broad spectrum of biological functions. A Human Phospho-Kinase Array Kit was used to simultaneously detect the relative

phosphorylation levels of 46 kinase phosphorylation sites in both NP-9 and NP-29 cell extracts 24 h after transducing cells with 10 MOI AdhCNT1. Levels of S473-phosphorylated Akt, S133-phosphorylated CREB (cAMP-response element-binding protein), T389-phosphorylated p70 S6 kinase and S63-phosphorylated c-Jun were increased compared with those in Adctrol-infected cells (Supplementary Figure S3). Interestingly, overexpression of hCNT1 induced a different phosphorylation profile in both cell lines compared with that observed for hCNT1 (Supplementary Figure S3).

An analysis of the time-course of the events following AdhCNT1 infection revealed an increase in Akt phosphorylation at both S473 and T308 sites, starting at 12 h after infection (Figure 5a). Erk phosphorylation was also potentiated at 18 h of AdhCNT1 infection in NP-9 cells, whereas increased Erk phosphorylation in AdhCNT1 NP-29-infected cells was only evident later (24 and 48 h after infection) (Figure 5a). Treatment with the Erk inhibitor PD98059 prevented Erk phosphorylation in both cell lines, although in hCNT1-overexpressing NP-29 cells, this treatment increased Akt S473 phosphorylation (Figure 5b). Moreover, NP-29 cells also appeared to show increased basal phosphorylation of Erk, as inferred from its status in Adctrol *versus* AdhCNT1-infected cells at the time of adenovirus removal (4 h; first assayed time-point). Interestingly, inhibition of Erk activation with PD98059 induced a slight but significant, reduction in hCNT1-associated cell death in NP-9, but not in NP-29, cells (Figure 5c). Inhibition of PI3K with wortmannin (20 and 100 nM) induced a slight decrease in hCNT1-induced phosphorylation of Akt at both S473 and T308 in NP-9 and NP-29 cells (Figure 5b), although no effect on cell viability was observed at 100 nM (Supplementary Figure S4).

hCNT1 effects are independent of its ability to translocate nucleosides. An imbalance in the four dNTP pools affects cell-cycle progression and has genotoxic consequences that may induce cell death. Thus, it could be argued that overexpression of a concentrative NT capable of translocating pyrimidine, but not purine, nucleosides could contribute to such an imbalance, thereby modifying cell

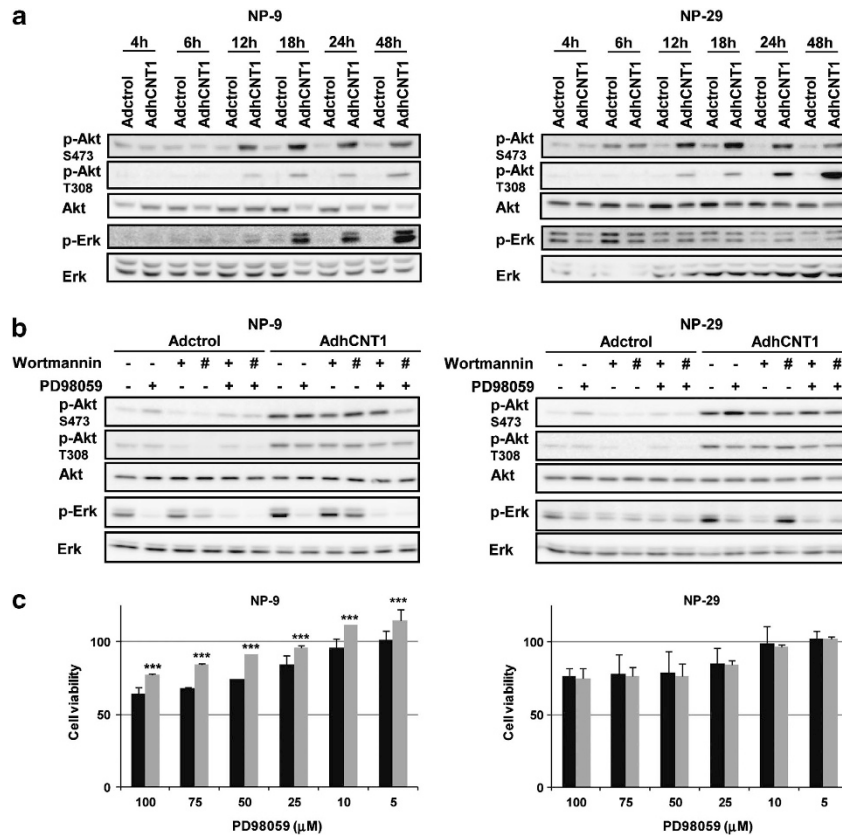


Figure 5 hCNT1 overexpression activates Akt and Erk. NP-9 and NP-29 cells were infected with AdhCNT1 or Adctrol at an MOI of 10. (a) The time-course of Akt and Erk phosphorylation was analysed in total cell extracts by western blotting using the indicated antibodies. (b) Infected NP-9 and NP-29 cells were treated with 50 μM PD98059 (MEK inhibitor) or 20 nM (+) or 100 nM (#) wortmannin (PI3K inhibitor) for 48 h. Total-cell lysates were analysed by immunoblotting with the indicated antibodies. (c) After infection with Adctrol (black bars) and AdhCNT1 (gray bars), NP-9 and NP-29 cells were treated with different concentrations of PD98059 and cell viability was assessed by MTT assay 72 h later. Data are expressed as percentage of viable cells relative to Adctrol- or AdhCNT1-infected cells. Results are means ± S.E.M. (*n* = 3). Statistical significance was determined with Student's *t*-test; ****P* < 0.005

physiology and cycling. This possibility was addressed by analysing the impacts of the polymorphic genetic variant hCNT1S546P on cell physiology of overexpression. This variant lacks nucleoside transport function, but apparently retains the ability to fold normally and insert into the plasma membrane.¹⁸ Forty-eight hours after infecting cells with an hCNT1S546P adenoviral vector (AdhCNT1SP) at an MOI of 10, no increase in cytidine uptake was observed; in contrast, upregulation of hCNT1-related activity was evident under the same experimental conditions in AdhCNT1-infected cells (Figure 6a). Interestingly, like AdhCNT1, AdhCNT1SP induced cell-cycle arrest at S phase in both NP-9 and NP-29 cells (Figure 6b). Similarly, Akt S473 and Erk phosphorylation were induced by both adenoviral constructs, with a concomitant increase in higher molecular weight forms of PARP (Figure 6c). To rule out the possibility that the effects triggered by hCNT1 and hCNT1SP are cell line specific, we infected two additional tumor pancreatic cell lines, Panc-1 and NP-18, and two breast cancer cell lines, T-47D and MDA-MB-468, with AdhCNT1 or the transport-null mutant AdhCNTSP. All cell lines showed clear activation of Akt S473 phosphorylation and increase in PARP molecular weight after hCNT1 or hCNT1SP transduction, whereas

changes in Erk phosphorylation proved to be more variable (Figure 6d).

Overexpression of hCNT1 or the transport-deficient hCNT1SP mutant alters cell migratory capacity. Despite the fact that hCNT1 affects cell-cycle progression and the Akt signaling pathway, the possibility that expression of this protein altered additional events capable of modulating tumor growth and invasiveness could not be ruled out. To address this issue, we conducted wound-healing assays on NP-9 cells infected with Adctrol, AdhCNT1, AdhCNT1SP or AdhENT1. Migration assays performed 24 h after infection showed that both hCNT1 and the transport-null hCNT1SP mutant promoted a significant decrease in migration (Figure 6e). No such effect was observed in cells infected with either Adctrol or an adenoviral vector overexpressing the NT hCNT1.

Discussion

This paper describes a novel and totally unexpected biological role for the NT protein hCNT1 that appears to be independent of its role as a mediator of nucleoside uptake by cells.

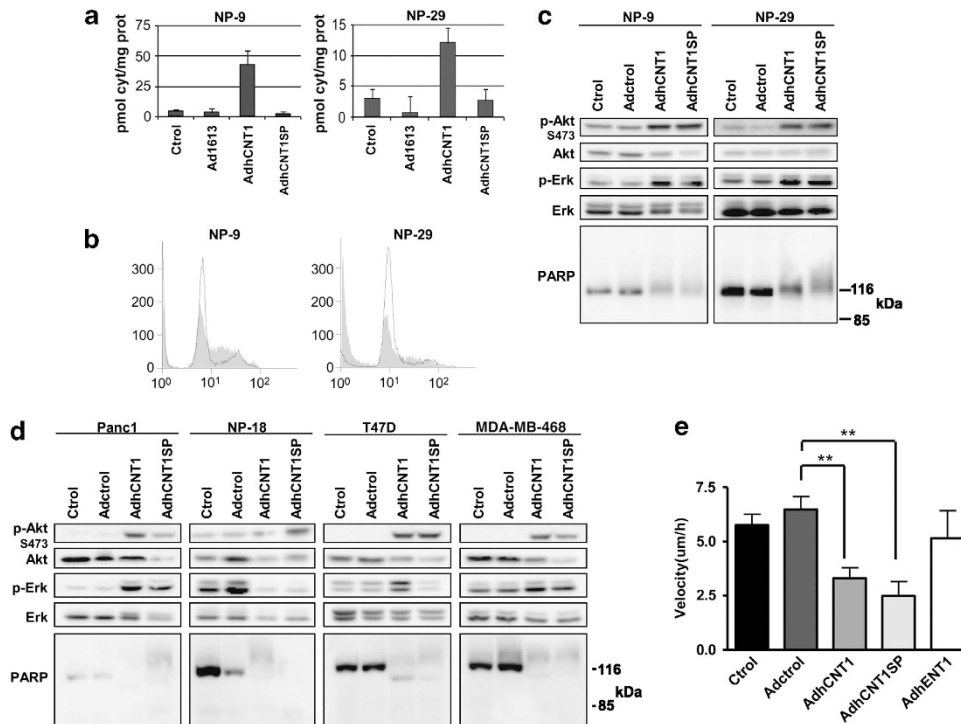


Figure 6 hCNT1SP mimics wild-type transporter outcomes. NP-9 and NP-29 cells were infected with Adctrol, AdhCNT1 or AdhCNT1SP at an MOI of 10, and all parameters were analysed 48 h post-infection. (a) hCNT1 sodium-dependent uptake of [³H]cytidine, calculated as uptake in NaCl medium minus uptake in choline chloride. Results are expressed as means ± S.E.M. and correspond to a representative experiment ($n = 3$). (b) Cell-cycle profile of NP-9 and NP-29 cells infected with Adctrol (black shape) or AdhCNT1SP (gray). (c) Western blot of total-cell lysates developed with the indicated antibodies. (d) Panc-1, NP-18, T-47D and MDA-MB-468 cells were individually infected with Adctrol, AdhCNT1 and AdhCNT1SP, and total cell lysates were analyzed by western blotting using the indicated antibodies. (e) NP-9 cell migration was examined by wound-healing assay 48 h after infection with Adctrol, AdhCNT1, AdhCNT1SP or AdhENT1. Migration speed was calculated as net displacement (μm)/time (h). Statistical significance was determined with Student's *t*-test; ** $P < 0.01$

This finding might represent a breakthrough in the field in the sense that, to date, a rationale for the apparent redundant expression of NTs in most cell types has been lacking, particularly considering that transporters often show overlapping or even identical selectivity profiles. Evidence supporting an additional role for particular transporters, as predicted by this study on hCNT1, could ultimately help to explain this apparent redundancy in transporter expression.

The existence of nutrient transceptors – transporter-like proteins with a receptor function – suggest that receptors for chemical signals may have been evolutionarily derived from nutrient transporters. Several examples of nutrient transporters with an additional signaling function, nutrient receptors with a transporter-like structure but without transport capacity, and G-protein-coupled receptors (GPCRs) that have nutrients as ligands are now available (reviewed in).¹⁹ hCNT1 seems to belong to this category of multifunctional proteins.

As introduced above, CNT1 is a highly regulated transporter protein.^{9–12} Reduced or even apparent loss of hCNT1 expression has been reported in a variety of human tumors, including breast, pancreatic and gynecological cancers.^{6–8,20} Furthermore, in hepatocellular carcinoma, despite highly variable expression, hCNT1 shows a trend towards reduced levels,^{21,22} whereas in hepatoblastoma and cholangiocarcinoma, hCNT1 mRNA levels are dramatically reduced compared with healthy liver.²²

The demonstration in this study of an hCNT1-related effect on cell-cycle progression is, in principle, consistent with the suggested role of this transporter protein in proliferating cells, which show an S phase-related increase in endogenous hCNT1 expression.¹² At that time of this latter study, it was postulated that this response could be related to the need for promoting nucleoside salvage for DNA synthesis. But the fact that the transport-null hCNT1SP mutant also promoted a similar effect predicts additional biological roles for this protein beyond the mere salvage of pyrimidine nucleosides.

Of particular interest is evidence that both hCNT1 and the mutated protein, hCNT1SP, promote PARP hyperactivation. Among other actions, PARP regulates chromatin organization, DNA repair, transcription and replication via PARylation or protein–protein interactions. Excessive DNA damage can also trigger a PARP-mediated cell death pathway, in which translocation of AIF to the nucleus has a central role. Activation of PARP can induce cell death by this mechanism, termed parthanatos, which differs from apoptosis, necrosis and autophagy.²³ Similar to parthanatos cell death, loss of cell membrane integrity and propidium iodide staining, as well as hyperactivation of PARP and subsequent accumulation of PAR polymers were observed upon hCNT1 overexpression. However, hCNT1-induced cell death was not associated with nuclear translocation of AIF.

Our results also showed that hCNT1 induced an early phosphorylation of Akt at Ser473 and T308 followed by Erk

activation. Surprisingly, activation of this canonical survival pathway by hCNT1 steered cells toward death, although Erk inhibition partially inhibited cell death only in NP-9 cells; in NP-29 cells, in which Erk inhibition provoked an increase in Akt Ser473 phosphorylation, it had no such effect. Moreover, wortmannin, a PI3K inhibitor, was unable to prevent cell death induced by hCNT1 overexpression in either cell lines.

It is well known that mTOR (mammalian target of rapamycin) has a pivotal role in cells, integrating diverse extra- and intracellular signals, and regulating cell growth, metabolism, survival and motility. mTOR is a common element of two functionally distinct complexes (mTORC1 and mTORC2) that regulate different sets of cellular responses. However, the roles of mTORC2 are not well established, and little is known about their upstream regulators. It has been reported that mTORC2 phosphorylates Akt on Ser473²⁴ and, together with Akt phosphorylation on Thr308 triggered by PDK1 (phosphoinositide-dependent kinase 1) in response to PI3K activation, confers full activity on Akt. However, the multiple lines of cross-talk towards other signaling cascades arising from mTORC2 are poorly understood, although our current results suggest a new pathway of Akt activation that involves the NT protein hCNT1.

Until recently, only mTORC1 had been reported to be regulated by nutrients such as amino acids.^{25–28} Interestingly, however, a very recent report indicated that the mTORC2 pathway is also activated in response to these nutrients.²⁹ Notably, NTs, like amino acid transporters, are located at the cell surface and might sense nutritional information; as such, they could contribute to the integration of extracellular and intracellular responses. The discovery of a signaling function in other transport proteins that were previously considered to be unfunctional transporters suggest that some transporter proteins behave as transceptors.¹⁹ Interestingly, the amino acid transporter SNAT2, a transceptor described in mammalian cells, exerts its signaling via mTOR.³⁰ Although the demonstration that a mutated transporter lacking nucleoside translocation ability was as effective as the wild-type protein in triggering selected effects on cell physiology is consistent with this concept, we cannot rule out the possibility of hCNT1SP-binding nucleosides but not transporting them into the cell. This possibility, although still speculative at this stage but currently under investigation, would illustrate the dual roles of nucleoside sensor and translocator played by hCNT1. Our current working hypothesis is that the N-terminal domain of hCNT1 contributes to the physiological responses reported here, thus putative protein partners that bind the N-terminal tail of hCNT1 are in the process of being identified. Interestingly, numerous putative interactors of the yeast transceptors, Gap1 and Mep2, have been recently characterized, allowing the two functions of the proteins to be unequivocally discriminated, confirming that transport is not required for signaling.³¹ Moreover, concomitantly with our work, it has been demonstrated the implication of human transporters in tumor progression in a transport-independent manner. The interaction of the human iodide transporter NIS with leukemia-associated RhoA guanine exchange factor (LARG) regulates cancer cell motility and invasiveness³² and sodium-coupled monocarboxylate transporter 1 (SMCT1) suppresses tumor progression through depletion of survivin.³³

Our demonstration that restoration of hCNT1 expression results in a variety of effects with potential relevance to tumor biology prompted us to revisit previous studies from our own laboratory. Among the previously collected data was information on hCNT1 expression that had been monitored by immunohistochemistry in nearly 300 gynecological tumors, including different subtypes of cervical, endometrial and ovarian cancers.⁸ Expression of hCNT1, hENT1 and hENT2 was analysed using tissue arrays. hCNT1 was the NT protein that most often showed null expression in a significant number of tumors. More importantly, this occurred preferentially in those histological subtypes known to be associated with poor prognosis, independent of therapy. More clinically oriented studies, in which hCNT1 loss is assessed in other types of tumors are now warranted.

In summary, a major finding of this work is that restoration of hCNT1 expression triggers intracellular responses affecting cell-cycle progression, cell migration and basal phosphorylation status of selected signaling kinases. Importantly, these effects are mimicked by a mutated transporter protein that lacks nucleoside translocation ability. Perhaps even more notable is the finding that hCNT1 introduction in an ectopic mouse model of human adenocarcinoma also resulted in significant inhibition of tumor growth. Thus, hCNT1 fits the profile of a transceptor and is likely to be relevant in tumor biology.

Materials and Methods

Reagents and antibodies. Dulbecco's modified Eagle's medium (DMEM), DMEM and F12 mixture (1:1) (DMEM-F12), RPMI-1640 medium, fetal bovine serum (FBS), trypsin and antibiotics were purchased from Gibco (Gibco, Grand Island, NY, USA). Anti-CNT1 antibody was raised and previously characterized in our laboratory. Anti-cyclin E and anti-Akt antibodies were obtained from Santa Cruz Biotechnology (Santa Cruz, CA, USA). The anti-PARP antibody was acquired from Becton Dickinson (San Diego, CA, USA). The anti-PAR antibody was purchased from Abcam (Cambridge, UK). Anti-phospho-Erk, anti-phospho-Akt (Ser473 and Thr308) and anti-Erk antibodies were purchased from Cell Signaling (Beverly, MA, USA). The anti-actin antibody was obtained from Sigma (St. Louis, MO, USA). The corresponding horseradish peroxidase (HRP)-conjugated secondary antibodies were purchased from DakoCytomation (Glostrup, Denmark). PD98059 and wortmannin were obtained from Calbiochem (Darmstadt, Germany), unless otherwise indicated.

Cell lines. NP-9, NP-29 and NP-18 cell lines were derived from human pancreatic adenocarcinomas that had been perpetuated as xenografts in nude mice.³⁴ PANC-1 (CRL-1469), 293 (CRL-1573), MCF7 (HTB-22), T-47D (HTB-133) and MDA-MB-4648 (HTB-132) cell lines were purchased from the American Type Culture Collection (ATCC, Promochem Partnership, Manassas, VA, USA). NP-9, NP-29 and MDA-MB-464 cell lines were maintained in DMEM-F12; NP-18, MCF7 and T-47D cell lines were maintained in RPMI-1640 medium; and PANC-1 and 293 cell lines were maintained in DMEM. All cell media were supplemented with 5% FBS and antibiotics, maintained at 37 °C in a humidified atmosphere containing 5% CO₂ and subcultured every 3–4 days. *Mycoplasma* assays, verification of morphology and growth curve analyses were performed routinely for all cell lines.

Adenoviral vector construction and infection conditions. Recombinant adenoviruses for Ad5CMV-hCNT1 (AdhCNT1) and Ad5CMV-hCNT1S546P (AdhCNT1SP) were generated by double recombination in bacterial cells. Briefly, hCNT1 and hCNT1S546P were cloned into a pShuttle-CMV plasmid, then recombinant adenoviruses were generated by cotransforming each transfer vector with the viral DNA plasmid p3602 into *Escherichia coli* strain BJ5183 (Stratagene, La Jolla, CA, USA). The recombinant adenoviral construct was then transfected into 293 cells to produce viral particles. Individual viral plaques were isolated and amplified in 293 cells, and recombinant adenoviruses containing hCNT1 or

hCNT1SP were identified by restriction enzyme digestion and PCR. The control adenovirus lacking an insert, Ad5CMV-1613 (Adctrol) and adenoviruses expressing equilibrative NTs were previously generated.^{35,36} All adenoviruses were propagated in 293 cells, and functional transduction units were determined using the hexon protein-staining technique.

Cells were seeded 24 h before adenovirus infection. Viral stocks, diluted to reach the desired MOI in medium supplemented with 5% FBS, were added to the cell monolayer. Mock-infected cells were incubated with the same medium. After 4 h, infection was stopped by replacing the medium.

RNA isolation and quantitative RT-PCR. Total RNA was isolated from cell lines using the SV Total RNA Isolation System (Promega, Madison, WI, USA). A total of 1 μ g of RNA was reverse transcribed to cDNA. Analyses of hCNT1 and GAPDH (internal control) mRNA levels were performed by RT-PCR using TaqMan Gene Expression Assays (Applied Biosystems, Carlsbad, CA, USA) as previously described by Molina-Arcas *et al.*³⁷ Relative quantification of gene expression was assessed using the $\Delta\Delta$ CT method, as described in the TaqMan user's manual (User Bulletin no. 2; Applied Biosystems). The amounts of mRNA were expressed as arbitrary units.

Nucleoside transport assay. Nucleoside uptake was measured as described previously³⁸ by exposing replicate cultures at room temperature to [³H] labeled cytidine (1 μ M, 1 μ Ci/ml; Perkin Elmer, Waltham, MA, USA) in sodium-containing or sodium-free transport buffer (137 mM NaCl or 137 mM choline chloride, 5 mM KCl, 2 mM CaCl₂, 1 mM MgSO₄, and 10 mM HEPES, pH 7.4). Initial rates of transport were determined using an incubation period of 1 min. Transport was stopped by washing with an excess volume of cold stop solution. Cells were then lysed in 100 μ l of 100 mM NaOH/0.5% Triton X-100. Aliquots were used for radioactivity counting and protein determination using the BCA reaction (Pierce, Rockford, IL, USA).

Western blot analysis. Cells were lysed in a buffer (20 mM Tris-HCl pH 8.0, 150 mM NaCl, 10 mM EDTA, 10 mM Na₄P₂O₇, 2 mM Na₃VO₄, 100 mM NaF, 1 mM B-glycerophosphate, 1% Igepal CA-630) containing 1% Complete Mini protease inhibitors (Roche, Mannheim, Germany) and 1% phosphatase inhibitors (Roche). Protein concentration in lysates was determined using the Bradford assay (Bio-Rad, Hercules, CA, USA). Proteins (20–30 μ g) in cell lysates were resolved by SDS-polyacrylamide gel electrophoresis on 12 or 8% gels and transferred to PVDF (polyvinylidene difluoride) membranes by standard methods. Membranes were immunoblotted with the indicated primary antibodies. Antibody labeling was detected using a chemiluminescence detection kit (Biological Industries, Kibbutz Beit Haemek, Israel).

Cell-cycle analysis. Infected cells were harvested and fixed with 70% ethanol (v/v) 72 h post-infection. After at least 24 h, cells were washed and resuspended in 0.5 ml of PBS containing RNase A (10 μ g/ml). Flow cytometry analyses were performed 1 h after the addition of propidium iodide (0.1 mg/ml) at room temperature using a Coulter XL (Beckman Coulter, Brea, CA, USA). Data from 10 000 cells were collected.

AnnexinV-FITC. Infected cells were harvested at 72 or 96 h post-infection and washed with 1% FBS in PBS. Then, cells were resuspended in binding buffer at a concentration of 5×10^5 – 1×10^6 cells, and 2.5 μ g/ml of annexinV-FITC and 5 μ g/ml of propidium iodide (Bender Medsystems, Burlingame, CA, USA) were added. Flow cytometry analyses were performed after 1 h incubation at room temperature in the dark using a Coulter XL (Beckman Coulter). Data from 10 000 cells were collected.

Immunofluorescence. Infected cells grown on uncoated glass coverslips were fixed for 15 min with 4% formaldehyde. Fixed cells were blocked by incubating with 5% normal serum and 0.3% Triton X-100 in PBS for 1 h at room temperature (RT), then incubated for 2 h at RT with rabbit anti-AIF antibody (Cell Signaling) in PBS containing 1% BSA and 0.3% Triton X-100. Secondary Alexa 488-conjugated anti-rabbit IgG (Molecular Probes; Eugene, OR, USA) was applied for 1 h at room temperature. Nuclei were counterstained with Hoechst 33342 (Sigma). Coverslips were mounted onto glass slides with aqua-poly/mount coverslipping medium (Polysciences Inc., Warrington, PA, USA). Images were captured using an SP11 laser-scanning confocal microscope fitted with the appropriate filters (Leica, Wetzlar, Germany).

Tumor growth studies. Tumor xenografts were developed by subcutaneous injection of 6×10^6 NP-9 cells into each posterior flank of female outbred nude mice (Charles River France, Lyon, France). Tumor volume was measured three times a week and was calculated according to the equation, $V(\text{mm}^3) = \pi/6 \times W \times L^2$, where L and W are length and width of the tumor, respectively. Once tumors reached 90 mm³, mice were randomized ($n = 7$ –10 per group) and cycles of intratumoral injections of Adctrol or AdhCNT1 (2×10^8 TU/20 μ l in PBS at 4 injection sites/tumor) were performed once a week for 3 weeks.

All animal procedures met the guidelines of European Community Directive 86/609/EEC and were previously approved by the Local Ethical Committee.

Kinase phosphorylation profile determination. A Human Phospho-Kinase Array Kit (R&D Systems, Minneapolis, MN, USA) was used to analyse the relative phosphorylation status of 46 kinases 24 h post-infection. All procedures were performed according to the manufacturer's instructions.

Cell viability assay. NP-9 and NP-29 cells were seeded at a density of 5000 cells/well in 96-well culture plates. Twenty-four hours after seeding, cultures were infected for 4 h and then exposed to different concentrations of PD98059 for 72 h. Viability was assessed using an MTT [3-(4,5-dimethylthiazol-2-yl)-2,5-diphenyl tetrazolium bromide] colorimetric assay (Sigma).

Cell migration assay. NP-9 cells were seeded in a six-well plate and infected 24 h later with Adctrol, AdhCNT1, AdhCNT1SP or AdhENT1 at an MOI of 10. Cultures were wounded 24 h later using a yellow pipette tip, washed twice to remove detached and damaged cells, and incubated overnight in fresh culture medium at 37 °C in a humidified 5% CO₂ atmosphere. Phase-contrast images were collected every 15 min using a Leica TS SP5 microscope with a $\times 10$ dry lens (Leica Microsystems). Images were subsequently analysed offline using ImageJ software (NIH, Bethesda, MD, USA), and migration speed was calculated as net displacement (μ m)/time (h).

Conflict of Interest

The authors declare no conflict of interest.

Acknowledgements. The authors would like to thank Ingrid Iglesias for excellent technical assistance. We also thank Dr. Miriam Molina-Arcas for her kind revision of the manuscript. This study has been supported by grants SAF2008-00577 and SAF2011-23660 (Ministerio de Ciencia e Innovación) and 2009SGR624 (Generalitat de Catalunya) to MP-A and by grant BIO2008-04692-C03-03 to AM. This laboratory belongs to the National Biomedical Research Institute on Liver and Gastrointestinal Diseases (CIBER EHD). SP-T and IH-R were CIBER researchers during the development of this study. CIBER is an initiative of the Instituto de Salud Carlos III (Ministerio de Ciencia e Innovación).

- Ritzel MW, Yao SY, Huang MY, Elliott JF, Cass CE, Young JD. Molecular cloning and functional expression of cDNAs encoding a human Na⁺ – nucleoside cotransporter (hCNT1). *Am J Physiol* 1997; **272**(2 Pt 1): C707–C714.
- Ritzel MW, Yao SY, Ng AM, Mackey JR, Cass CE, Young JD. Molecular cloning, functional expression and chromosomal localization of a cDNA encoding a human Na⁺ /nucleoside cotransporter (hCNT2) selective for purine nucleosides and uridine. *Mol Membr Biol* 1998; **15**: 203–211.
- Ritzel MW, Ng AM, Yao SY, Graham K, Loewen SK, Smith KM *et al.* Molecular identification and characterization of novel human and mouse concentrative Na⁺ – nucleoside cotransporter proteins (hCNT3 and mCNT3) broadly selective for purine and pyrimidine nucleosides (system cib). *J Biol Chem* 2001; **276**: 2914–2927.
- Govindarajan R, Bakken AH, Hudkins KL, Lai Y, Casado FJ, Pastor-Anglada M *et al.* *In situ* hybridization and immunolocalization of concentrative and equilibrative nucleoside transporters in the human intestine, liver, kidneys, and placenta. *Am J Physiol Regul Integr Comp Physiol* 2007; **293**: R1809–R1822.
- Lane J, Martin TA, McGuigan C, Mason MD, Jiang WG. The differential expression of hCNT1 and hENT1 in breast cancer and the possible impact on breast cancer therapy. *J Exp Ther Oncol* 2010; **8**: 203–210.
- Gloeckner-Hofmann K, Guillen-Gomez E, Schmidtgen C, Porstmann R, Ziegler R, Stoss O *et al.* Expression of the high-affinity fluoropyrimidine-preferring nucleoside transporter hCNT1 correlates with decreased disease-free survival in breast cancer. *Oncology* 2006; **70**: 238–244.

7. Bhutia YD, Hung SW, Patel B, Lovin D, Govindarajan R. CNT1 expression influences proliferation and chemosensitivity in drug-resistant pancreatic cancer cells. *Cancer Res* 2011; **71**: 1825–1835.
8. Farre X, Guillen-Gomez E, Sanchez L, Hardisson D, Plaza Y, Lloberas J *et al*. Expression of the nucleoside-derived drug transporters hCNT1, hENT1 and hENT2 in gynecologic tumors. *Int J Cancer* 2004; **112**: 959–966.
9. Podgorska M, Kocbuch K, Grden M, Szulc A, Szutowicz A, Pawelczyk T. Different signaling pathways utilized by insulin to regulate the expression of ENT2, CNT1, CNT2 nucleoside transporters in rat cardiac fibroblasts. *Arch Biochem Biophys* 2007; **464**: 344–349.
10. Klein K, Kullak-Ublick GA, Wagner M, Trauner M, Eloranta JJ. Hepatocyte nuclear factor-4alpha and bile acids regulate human concentrative nucleoside transporter-1 gene expression. *Am J Physiol Gastrointest Liver Physiol* 2009; **296**: G936–G947.
11. Fernandez-Veledo S, Valdes R, Wallenius V, Casado FJ, Pastor-Anglada M. Up-regulation of the high-affinity pyrimidine-preferring nucleoside transporter concentrative nucleoside transporter 1 by tumor necrosis factor-alpha and interleukin-6 in liver parenchymal cells. *J Hepatol* 2004; **41**: 538–544.
12. Valdes R, Casado FJ, Pastor-Anglada M. Cell-cycle-dependent regulation of CNT1, a concentrative nucleoside transporter involved in the uptake of cell-cycle-dependent nucleoside-derived anticancer drugs. *Biochem Biophys Res Commun* 2002; **296**: 575–579.
13. Lu H, Chen C, Klaassen C. Tissue distribution of concentrative and equilibrative nucleoside transporters in male and female rats and mice. *Drug Metab Dispos* 2004; **32**: 1455–1461.
14. Soler C, Garcia-Manteiga J, Valdes R, Xaus J, Comalada M, Casado FJ *et al*. Macrophages require different nucleoside transport systems for proliferation and activation. *Faseb J* 2001; **15**: 1979–1988.
15. Aymerich I, Pastor-Anglada M, Casado FJ. Long term endocrine regulation of nucleoside transporters in rat intestinal epithelial cells. *J Gen Physiol* 2004; **124**: 505–512.
16. Pennycooke M, Chaudary N, Shuralyova I, Zhang Y, Coe IR. Differential expression of human nucleoside transporters in normal and tumor tissue. *Biochem Biophys Res Commun* 2001; **280**: 951–959.
17. Bock AJ, Dong HP, Trope CG, Staff AC, Risberg B, Davidson B. Nucleoside transporters are widely expressed in ovarian carcinoma effusions. *Cancer Chemother Pharmacol* 2012; **69**: 467–475.
18. Cano-Soldado P, Gorraitz E, Errasti-Murugarren E, Casado FJ, Lostao MP, Pastor-Anglada M. Functional analysis of the human concentrative nucleoside transporter-1 variant hCNT1S546P provides insight into the sodium-binding pocket. *Am J Physiol Cell Physiol* 2012; **302**: C257–C266.
19. Thevelein JM, Voordeckers K. Functioning and evolutionary significance of nutrient transporters. *Mol Biol Evol* 2009; **26**: 2407–2414.
20. Lane J, Martin TA, McGuigan C, Mason MD, Jiang WG. The differential expression of hCNT1 and hENT1 in breast cancer and the possible impact on breast cancer therapy. *J Exp Ther Oncol* 8: 203–210.
21. Zollner G, Wagner M, Fickert P, Silbert D, Fuchsichler A, Zatloukal K *et al*. Hepatobiliary transporter expression in human hepatocellular carcinoma. *Liver Int* 2005; **25**: 367–379.
22. Martinez-Becerra P, Vaquero J, Romero MR, Lozano E, Anadon C, Macias RI *et al*. No correlation between the expression of FXR and genes involved in multidrug resistance phenotype of primary liver tumors. *Mol Pharm* 2012; **9**: 1693–1704.
23. Harraz MM, Dawson TM, Dawson VL. Advances in neuronal cell death 2007. *Stroke* 2008; **39**: 286–288.
24. Sarbassov DD, Guertin DA, Ali SM, Sabatini DM. Phosphorylation and regulation of Akt/PKB by the rictor-mTOR complex. *Science* 2005; **307**: 1098–1101.
25. Wullschlegler S, Loewith R, Hall MN. TOR signaling in growth and metabolism. *Cell* 2006; **124**: 471–484.
26. Laplante M, Sabatini DM. mTOR signaling at a glance. *J Cell Sci* 2009; **122**(Pt 20): 3589–3594.
27. Bhaskar PT, Hay N. The two TORCs and Akt. *Dev Cell* 2007; **12**: 487–502.
28. Nicklin P, Bergman P, Zhang B, Triantafellow E, Wang H, Nyfeler B *et al*. Bidirectional transport of amino acids regulates mTOR and autophagy. *Cell* 2009; **136**: 521–534.
29. Tato I, Bartrons R, Ventura F, Rosa JL. Amino acids activate mammalian target of rapamycin complex 2 (mTORC2) via PI3K/Akt signaling. *J Biol Chem* 2011; **286**: 6128–6142.
30. Pinilla J, Aledo JC, Cwiklinski E, Hyde R, Taylor PM, Hundal HS. SNAT2 transceptor signalling via mTOR: a role in cell growth and proliferation? *Front Biosci (Elite Ed)* 2011; **3**: 1289–1299.
31. Van Zeebroeck G, Kimpe M, Vandormael P, Thevelein JM. A split-ubiquitin two-hybrid screen for proteins physically interacting with the yeast amino acid transceptor Gap1 and ammonium transceptor Mep2. *PLoS One* 2011; **6**: e24275.
32. Lacoste C, Herve J, Bou Nader M, Dos Santos A, Moniaux N, Valogne Y *et al*. Iodide transporter NIS regulates cancer cell motility and invasiveness by interacting with the Rho guanine nucleotide exchange factor LARG. *Cancer Res* 2012; **72**: 5505–5515.
33. Coothankandaswamy V, Elangovan S, Singh N, Prasad PD, Thangaraju M, Ganapathy V. The plasma membrane transporter SLC5A8 suppresses tumor progression through depletion of survivin without involving its transport function. *Biochem J* 2012; **450**: 169–178.
34. Villanueva A, Garcia C, Paules AB, Vicente M, Megias M, Reyes G *et al*. Disruption of the antiproliferative TGF-beta signaling pathways in human pancreatic cancer cells. *Oncogene* 1998; **17**: 1969–1978.
35. Cascallo M, Calbo J, Capella G, Fillat C, Pastor-Anglada M, Mazo A. Enhancement of gemcitabine-induced apoptosis by restoration of p53 function in human pancreatic tumors. *Oncology* 2005; **68**: 179–189.
36. Perez-Torras S, Garcia-Manteiga J, Mercade E, Casado FJ, Carbo N, Pastor-Anglada M *et al*. Adenoviral-mediated overexpression of human equilibrative nucleoside transporter 1 (hENT1) enhances gemcitabine response in human pancreatic cancer. *Biochem Pharmacol* 2008; **76**: 322–329.
37. Molina-Arcas M, Bellosillo B, Casado FJ, Montserrat E, Gil J, Colomer D *et al*. Fludarabine uptake mechanisms in B-cell chronic lymphocytic leukemia. *Blood* 2003; **101**: 2328–2334.
38. del Santo B, Valdes R, Mata J, Felipe A, Casado FJ, Pastor-Anglada M. Differential expression and regulation of nucleoside transport systems in rat liver parenchymal and hepatoma cells. *Hepatology* 1998; **28**: 1504–1511.



Cell Death and Disease is an open-access journal published by **Nature Publishing Group**. This work is licensed under a **Creative Commons Attribution-NonCommercial-ShareAlike 3.0 Unported License**. To view a copy of this license, visit <http://creativecommons.org/licenses/by-nc-sa/3.0/>

Supplementary Information accompanies this paper on Cell Death and Disease website (<http://www.nature.com/cddis>)